

Integrated FPI-FBG composite all-fiber sensor for simultaneous measurement of liquid refractive index and temperature

Ying-gang Liu^{a,*}, Xin Liu^a, Ting Zhang^a, Wei Zhang^b

^a Key Laboratory of Photoelectricity Gas & Oil Logging and Detecting of Ministry of Education, Xi'an Shiyou University, Xi'an 710065, China

^b School of Environmental and Municipal Engineering, Xi'an University of Architecture and Technology, Xi'an 710055, China

ARTICLE INFO

Keywords:

Optical fiber sensor
Fabry–Perot interferometer
Fiber Bragg grating
Refractive index
Temperature
Excimer laser

ABSTRACT

A miniature and all-optical fiber sensor based on integration of Fabry–Perot interferometer (FPI) and fiber Bragg grating (FBG) is proposed and experimentally demonstrated for simultaneous measurement of refractive index (RI) and temperature in this paper. The integrated FPI-FBG composite fiber sensor is constructed by manufacturing a micro-hole in FBG, where two parallel reflecting surfaces of micro-hole perform as cavity mirrors of FPI. Experimental results show that the temperature and RI sensitivity of spectral dip wavelength for FPI are $-0.189 \text{ nm}/^\circ\text{C}$ and $1210.490 \text{ nm}/\text{RIU}$, respectively. The temperature sensitivity for FBG is $0.011 \text{ nm}/^\circ\text{C}$, and the FBG is insensitive to RI. Using these different sensitivities, a matrix can be constructed and used in simultaneous measurement of RI and temperature. The resolutions of $0.1 \text{ }^\circ\text{C}$ and $1.5 \times 10^{-5} \text{ RIU}$ can be obtained. Owing to compact size in dimensions, the sensor can be used to measure RI and temperature simultaneously in tiny liquid environment.

1. Introduction

As an important parameter for sensing, refractive index (RI) has been widely used in the field of industrial production, environmental monitoring, clinical testing, and food inspection [1]. But RI measurement is inevitably affected by temperature changes, so it is necessary to achieve simultaneous measurement of RI and temperature. In recent years, optical fiber sensors, such as Mach–Zehnder interferometer (MZI) [2,3], Michelson interferometer [4,5], Fabry–Perot interferometer (FPI) [6–10] and fiber Bragg grating (FBG) [11–13], have attracted much attention in applications for monitoring various physical quantities. Integration [11,12,14], all-optical fiber [15–18], micromatation [16–19] and multi-parameter measurement [11, 20,21] are main directions for development of fiber optic sensor technology. J. Xia [12] presented a magnetic field sensor based on a magnetic fluid-filled FP-FBG structure. The FBG was written on the insert fiber end of FP cavity and acted as a temperature compensation unit, where the FBG and FP cavity are connected by capillary tube, so that the cross-sensitivity effect of the temperature and magnetic field could be overcome in magnetic field measurement. A multi-parameter sensor based on a tilted fiber Bragg grating for performing simultaneous measurement of strain, temperature, and RI was demonstrated by N. J. Alberto [13]. The resolutions are $5.7 \times 10^{-4} \text{ RIU}$, $4 \text{ } \mu\text{e}$ and $0.5 \text{ }^\circ\text{C}$ for RI, strain and temperature, respectively. Literature [15] fabricated an all-fiber sensor which contains a MZI and a FBG. The MZI was made up of core-offset structure and spherical-shape structure.

This structure has some advantages, such as low fabrication cost and good linearity, but complicated configuration creates limitations for its applications.

In this paper, we propose and fabricate an integrated FPI-FBG composite fiber sensor, which isn't cascading FPI and FBG but integrating FPI in FBG by excimer laser machining method. Due to having different responses for RI and temperature, we can realize simultaneous measurement of temperature and RI using sensitivity matrix. Compared with mentioned sensors, the advantages of sensor we proposed are compact structure, low fabrication cost, and micromatation.

2. Fabrication and sensing principle

For the fabrication processes of our proposed integrated FPI-FBG composite fiber sensor, the schematic diagrams are shown in Fig. 1, and there are four main steps. In experiments, we firstly need to fabricate a FBG, and then machine a micro-hole cavity in FBG. The FBG used in this experiment was obtained by using ultraviolet light to irradiate single-mode fiber (SMF) ($9 \text{ } \mu\text{m}/125 \text{ } \mu\text{m}$, ChangFei, China) with phase mask method. The power, center wavelength, frequency, and repetition rate of employed Excimer laser (ATLEX-500, ATL, Germany) are 30 mJ, 193 nm, 300 Hz, and 50 Hz, respectively. During the course of micro-hole fabrication, a charge-coupled diode (CCD) camera is employed to obtain the image of optical fiber and monitor the inscription of fiber. At first, both ends of FBG are stretched out and fixed on a glass slide, and

* Corresponding author.

E-mail address: ygliu@xsyu.edu.cn (Y.-g. Liu).

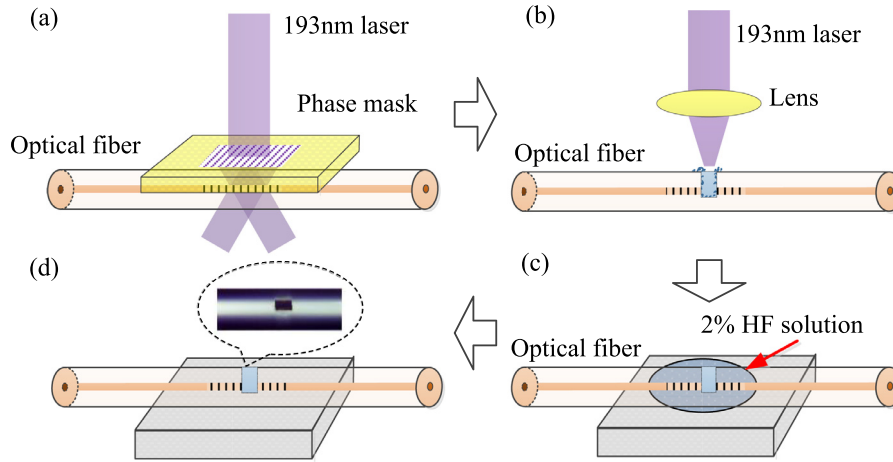


Fig. 1. Schematic diagrams of production process for the integrated FPI-FBG composite fiber sensor.
 (a) Fabrication of single-mode fiber Bragg grating with phase mask method.
 (b) Machining micro-hole with 193 nm laser in the midpoint of FBG.
 (c) Cleaning micro-hole with 2% HF solution.
 (d) Optical microscope overlooking image of micro-hole after cleanout.

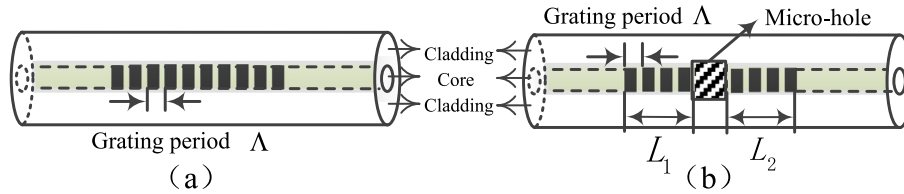


Fig. 2. Schematic diagram of the sensor.
 (a) Schematic diagram of fiber Bragg grating.
 (b) Schematic diagram of integrated FPI-FBG composite fiber sensor.

then the whole is placed on a precise tunable three-dimensional micro-displacement platform (10 μm, China). Next, we adjust the X, Y axis of platform to make FBG located on the view field of microscope, and we adjust Z axis to make laser spot focus on the FBG. After those steps, we choose carving way of rectangular hole and begin to fabricate the sensor. We open the control switch and let the laser irradiate fiber for 15 s. Once time is enough for machining a through-out micro-hole, we stop the irradiation and remove the fiber from the platform. Then, the 2% solution of hydrofluoric acid is used to clean the machined holes before measurement, so that the chippings in micro-holes can be cleared up. Finally, we clean the integrated FPI-FBG structure with deionized water to prevent excessive corrosion. As all the above steps are finished, the integrated FPI-FBG composite fiber sensor with a high-quality resonant cavity is fabricated successfully.

Fig. 2(a) shows the schematic diagram of FBG. The shadings in diagram indicate periodic variation of RI, which is called grating period. When a micro-hole is fabricated in FBG, it will lead to an abrupt phase change, which divides FBG into two sections, as shown in Fig. 2(b). L_1 and L_2 are defined as length of each section, respectively. The magnitude of phase shift produced from micro-hole can be expressed as

$$\varphi = \frac{4\pi nL}{\lambda} \quad (1)$$

where n is the RI of cavity and L is the length of cavity, respectively. The rectangles in shaded section represent the micro-hole which is carved in the midpoint of FBG.

The two parallel surfaces of micro-hole perform as cavity mirrors of FPI. The free spectrum range (FSR) of interference spectrum can be expressed as [17]

$$FSR = \frac{\lambda^2}{2nL} \quad (2)$$

During the course of experiment, the micro-hole is fabricated in the midpoint of FBG, and the length of micro-hole is 60.40 μm, which is corresponding to the FSR of 14.92 nm in water with refractive index of 1.333. The length of FBG is 1.5 cm.

Fig. 3(a) shows the reflective spectrum of proposed sensor, and Fig. 3(b) shows the detailed figure of FBG. We can see that the introduction of phase shift can open a transmission window at the wavelength of 1553.445 nm, as arrow point to in Fig. 3(b), in reflective spectrum of FBG [22]. A fast Fourier transform (FFT) on the spectrum in Fig. 3(a) is carried out, and the optical path difference (OPD) is determined based on the FFT results. The relationship between OPD and the length of cavity can be expressed as

$$OPD = 2nL \quad (3)$$

We can calculate that the length of cavity is 60.05 μm, which is very in accord with the measurement value.

As ambient temperature and RI change, the working mechanism of sensor for simultaneous measurement of RI and temperature is as follows. The response of FPI to temperature and RI can be expressed as

$$\Delta\lambda_{Dip-FPI} = k_{T_1}\Delta T + k_{n_1}\Delta n \quad (4)$$

where $\Delta\lambda_{Dip-FPI}$ is the wavelength shift of one spectral dip of FPI, k_{T_1} and k_{n_1} are the sensitivity coefficients of temperature and RI for interference dip of FPI, and ΔT and Δn are the variations of temperature and RI, respectively. Similarly, the response of FBG also can be expressed as

$$\Delta\lambda_{Peak-FBG} = k_{T_2}\Delta T + k_{n_2}\Delta n \quad (5)$$

where $\Delta\lambda_{Peak-FBG}$ is peak wavelength shift of FBG. k_{T_2} and k_{n_2} are the sensitivity peak coefficients of temperature and RI for reflection peak wavelength of FBG. Owing to the fact that k_{T_1} is unequal to k_{T_2} , and k_{n_1} is

Download English Version:

<https://daneshyari.com/en/article/11003703>

Download Persian Version:

<https://daneshyari.com/article/11003703>

[Daneshyari.com](https://daneshyari.com)